

Stochastic Control through Approximate Bayesian Input Inference

Joe Watson, Hany Abdulsamad, Rolf Findeisen, *Member, IEEE*, and Jan Peters, *Fellow, IEEE*

Abstract—Optimal control under uncertainty is a prevailing challenge in control, due to the difficulty in producing tractable solutions for the stochastic optimization problem. By framing the control problem as one of input estimation, advanced approximate inference techniques can be used to handle the statistical approximations in a principled and practical manner. Analyzing the Gaussian setting, we present a solver capable of several stochastic control methods, and was found to be superior to popular baselines on nonlinear simulated tasks. We draw connections that relate this inference formulation to previous approaches for stochastic optimal control, and outline several advantages that this inference view brings due to its statistical nature.

Index Terms—Stochastic Optimal Control, Approximate Inference

I. INTRODUCTION

Control-as-inference [1]–[4] refers to the formulation of the control problem as inference of an appropriate probabilistic graphical model (PGM). The motivation for this perspective is threefold: Firstly, it allows one to derive intriguing mathematical dualities between the two disciplines, which has captivated researchers for decades [5]–[7]. Secondly, in making the effort to reframe the optimal control problem as one of Bayesian inference, we gain access to a sophisticated suite of tools and insights developed by the statistics community, that provide value in both theory and practice [8]. In particular, as stochasticity presents a challenge in designing tractable algorithms for control [9], the statistics community have developed several methods for solving stochastic problems through principled approximations. Finally, an abundance of data, combined with the pervasive demand for sophisticated control design, has driven the study of *learning* for control, where experience is leveraged within the control optimization process [10], [11]. Given this setting, the motivation of inference-based optimal control is clear, as an inference-based solver is complementary to a learned statistical dynamics model, and could be applied to reason about data directly in a model-free fashion. Using the common language of inference, optimal control and data can be integrated directly to synthesize effective control learning algorithms [12].

This paper consolidates preliminary work [13], [14], which expands upon and analyzes the Gaussian message passing

This article was submitted for review on May 14th 2021. This project has received funding from the European Union’s Horizon 2020 program under grant agreement No #640554 (SKILLS4ROBOTS).

J. Watson, H. Abdulsamad and J. Peters are with the Intelligent Autonomous Systems group, Technical University of Darmstadt, Germany (correspondence: joe@robot-learning.de).

R. Findeisen is with the Laboratory for Systems Theory and Automatic Control, Otto-von-Guericke University Magdeburg, Germany.

view of control. Specifically, it builds on the view of optimal control as the problem of input estimation [15] through message passing on a probabilistic graphical model [16], [17], which enables computation of control laws within a Bayesian formalism. We propose an expectation maximization (EM) approach that enables the optimization of priors and hyperparameters, which is crucial for successfully applying these methods to complex control tasks which require iterative control evaluation and optimization. This is in contrast to prior work, which is limited to fixed priors and hyperparameters, and relies on iterated inference of the state distribution rather than EM on the state-action distribution [17]. Moreover, this article also presents a novel derivation of the control-inference duality through the state-action value function, and provides analysis and extensions of this method inspired by stochastic control. While our inference-based approach may appear unintuitive as an optimal control method, we are able to ground the approach in the prior control literature by relating it to aspects of risk-sensitive, maximum entropy and dual control. We show these advances, which improve accuracy, exploration and regularization, result in superior performance compared to popular baseline solvers on simulated environments.

The rest of this article is organized as follows, Section II provides the necessary background on stochastic optimal control. Section III describes the core control-as-inference framework, and Section IV discusses extensions inspired by and relevant to stochastic control.

A. Notation

\mathbf{X}_1^T denotes a sequence of vectors $\{\mathbf{x}_1, \dots, \mathbf{x}_T\}$. For vectors $\mathbf{x}_1, \mathbf{x}_2$ and matrix $\mathbf{S} \succ 0$ we define $\|\mathbf{x}_1 - \mathbf{x}_2\|_{\mathbf{S}}^2 = (\mathbf{x}_1 - \mathbf{x}_2)^T \mathbf{S} (\mathbf{x}_1 - \mathbf{x}_2)$. The probability of event X is denoted by $\text{Pr}(X)$. The expression $\mathbf{x} \sim p(\mathbf{x})$ means that a random variable $\mathbf{x} \in \mathbb{R}^n$ is distributed according to the distribution $p(\mathbf{x})$. The log-likelihood under this distribution is expressed as $\mathcal{L}(\mathbf{x}) = \log p(\mathbf{x})$. $\mathcal{N}(\boldsymbol{\mu}, \boldsymbol{\Sigma})$ is a multivariate Normal distribution with mean $\boldsymbol{\mu} \in \mathbb{R}^n$ and covariance $\boldsymbol{\Sigma} \in \mathbb{S}_+^n$ where $+$ denotes positive (semi)-definiteness. Normal and Gaussian are used interchangeably to refer to this distribution, and it is also presented in its canonical form $\mathcal{N}[\boldsymbol{\nu}, \boldsymbol{\Lambda}]$, where $\boldsymbol{\Lambda} = \boldsymbol{\Sigma}^{-1}$ and $\boldsymbol{\nu} = \boldsymbol{\Lambda}\boldsymbol{\mu}$. For a random variable \mathbf{x} , $\mathbb{E}[\mathbf{x}]$ and $\mathbb{V}[\mathbf{x}]$ denote the mean and variance.

B. Related Work

Control-as-inference has been considered since the conception of modern optimal control, due to the concurrent

development of LQR, Kalman filtering and LQG [5], [18].

The revival in control-as-inference stems from work on path integral [4], [19], trans-dimensional Markov chain Monte Carlo [20], linearly-solveable Markov decision process [21] and message passing [16], [22] methods. While dissimilar in motivation and implementation, these methods have many shared assumptions and qualities [23]. This inference-view was inspired in part by reinforcement learning, which requires both optimal control and statistical methods [3], [22], [24]–[26], as well as accelerating solvers based on differential dynamic programming (DDP) [27] through Bayesian methods [16], [17]. Furthermore, trajectory optimization has been regularized using information-geometric constraints, such as the Kullback-Liebler divergence [28]–[30], which can be interpreted as variational inference [31]. Inference methods have also been adopted for motion planning [32], applying optimized factor graph solvers to planning tasks [33].

Many ideas presented here, motivated from the inference view, have been previously applied purely in a control context. Extended LQR incorporates a filtering-like forward optimization into iLQR, [34], [35]. Quadrature methods have been adopted for trajectory optimization for greater accuracy [36]–[39]. Sampled DDP [40], [41] uses Monte Carlo rollouts to accurately estimate value functions of non-smooth dynamics.

II. STOCHASTIC CONTROL

In this section, we review relevant topics from stochastic optimal control. These topics are outlined in order to identify how inference performs optimal control. Specifically, we connect risk-sensitive linear quadratic dynamic programming to linear Gaussian Bayesian smoothing.

A. Finite-Horizon, Discrete-Time Optimal Control

We consider a stochastic, discrete-time, fully-observed, non-linear, time-varying dynamical system, f_t , with state $x \in \mathbb{R}^{d_x}$ and input $u \in \mathbb{R}^{d_u}$. Given this system, we desire the optimal controls over a time horizon T that minimizes the time-varying cost functions $C_t : \mathbb{R}^{d_x} \times \mathbb{R}^{d_u} \rightarrow \mathbb{R}$ in expectation over the stochastic dynamics,

$$\begin{aligned} \min_{U_1^{T-1}} \quad & \mathbb{E}[C_T(x_T) + \sum_{t=1}^{T-1} C_t(x_t, u_t)] \\ \text{s.t.} \quad & x_{t+1} = f_t(x_t, u_t) + \eta_t, \quad \eta_t \sim \mathcal{N}(\mathbf{0}, \Sigma_{\eta_t}). \end{aligned} \quad (1)$$

The dynamic programming solution introduces the time-varying state and state-action value functions V and Q , where

$$\begin{aligned} V_t(x) &= \min_u Q_t(x_t, u_t), \quad V_T(x_T) = C_T(x_T), \text{ and} \\ Q_t(x_t, u_t) &= \mathbb{E}[C_t(x_t, u_t) + V_{t+1}(f_t(x_t, u_t))]. \end{aligned} \quad (2)$$

We summarize the linear quadratic Gaussian (LQG [42]) dynamic programming solution using the Q function. These expressions are required for identifying the inference relations in the linear Gaussian setting. For compactness, we introduce state-action vector τ , where $\tau = [x \ u]^\top \in \mathbb{R}^{d_\tau}$.

In the case of LQR, the cost function is quadratic,

$$\begin{aligned} C_t(x, u) &= c_t + c_t^\top \begin{bmatrix} x \\ u \end{bmatrix} + \begin{bmatrix} x \\ u \end{bmatrix}^\top \begin{bmatrix} C_{xx_t} & C_{xu_t} \\ C_{xu_t}^\top & C_{uu_t} \end{bmatrix} \begin{bmatrix} x \\ u \end{bmatrix}, \\ &= \tau^\top C_t \tau + c_t^\top \tau + c_t, \text{ where } C_t \succ 0 \ \forall t. \end{aligned}$$

The state-action value function is also quadratic,

$$\begin{aligned} Q_t(x_t, u_t) &= q_t + q_t^\top \begin{bmatrix} x_t \\ u_t \end{bmatrix} + \begin{bmatrix} x_t \\ u_t \end{bmatrix}^\top \begin{bmatrix} Q_{xx_t} & Q_{xu_t} \\ Q_{ux_t} & Q_{uu_t} \end{bmatrix} \begin{bmatrix} x_t \\ u_t \end{bmatrix} \\ &= q_t + q_t^\top \tau_t + \tau_t^\top Q_t \tau_t, \end{aligned}$$

as is the value function, $V_t(x_t) = v_t + v_t^\top x_t + x_t^\top V_t x_t$. The dynamics are affine Gaussian in the state,

$$x_{t+1} = F_t \begin{bmatrix} x_t \\ u_t \end{bmatrix} + \bar{f}_t + \eta_t, \text{ where } F_t = [F_{x_t} \ F_{u_t}]. \quad (4)$$

The Q function update, (3), becomes

$$q_t = c_t + v_{t+1} F_{t+1}, \quad Q_t = C_t + F_{t+1}^\top V_{t+1} F_{t+1}. \quad (5)$$

Using Q , the optimal control is $u_t^* = \arg \min_u Q_t(x_t, u_t)$,

$$u_t^* = -Q_{uu_t}^{-1}(q_{u_t} + Q_{ux_t} x_t) = K_t x_t + k_t = \pi_t(x_t), \quad (6)$$

yielding a time-varying linear control law (TV-LC). Substituting equation (6) into (2), the value function updates are

$$v_t = q_{x_t} - q_{u_t}^\top Q_{uu_t}^{-1} Q_{ux_t}, \quad V_t = Q_{xx_t} - Q_{xu_t} Q_{uu_t}^{-1} Q_{ux_t}. \quad (7)$$

The above summary also corresponds to differential dynamic programming when the cost and dynamics are updated with a second-order Taylor approximation each iteration. However, the assumption of time-varying affine dynamics correspond to the Gauss-Newton approximation (iLQR) [43], [44].

B. Risk-Sensitive Control

Introduced by Jacobson, risk-sensitive linear exponential quadratic Gaussian (LEQG) control [45], [46] derives a policy that, unlike LQG, is dependent on the severity of uncertainty in the system dynamics. This sensitivity is determined by the scaling parameter σ in the transformed objective,

$$-\frac{1}{\sigma} \log \mathbb{E} \left[\exp \left(-\sigma \left[C_T(x_T) + \sum_{t=0}^{T-1} C_t(x_t, u_t) \right] \right) \right], \quad (8)$$

which results in the adjusted Bellman equation,

$$Q_t^\sigma(x_t, u_t) = C_t(x_t, u_t) + \frac{1}{\sigma} \log \mathbb{E}[\exp(-\sigma V_{t+1}(x_{t+1}))].$$

The expectation results in a transformed value function V^σ

$$\exp(-\sigma V^\sigma(x)) = \int \exp(-\sigma V(x)) \mathcal{N}(x; \mu_x, \Sigma_\eta) dx.$$

For a quadratic model of V (equation 4), this expectation is equivalent to adding two Gaussian random variables, so $V_t^\sigma = (\Sigma_{\eta_t} + \frac{1}{\sigma} V_t^{-1})^{-1}$. The Q function naturally has a similar adjustment, $Q_t^\sigma = C_t + F_{t+1}^\top V_t^\sigma F_{t+1}$. Due to these transforms, the risk-sensitive optimal policy depends on the disturbance covariance. For $\sigma > 0$, the behavior is ‘risk seeking’, which attenuates the controls. For $\sigma < 0$, the behavior is ‘risk averse’ and the gains are amplified. As $\sigma \rightarrow 0$, we recover the nominal behavior, referred to as risk neutral. The risk-sensitive objective can be optimized through linearization for nonlinear systems [47]. In practice, the risk-averse case is preferred to amplify the feedback and reduce variance.

C. The Gaussian Assumption

For tractability and convenience, we assume a Gaussian state-action distribution for the remainder of this article. This assumption posits a unimodal state-action distribution, which is reasonable for a weakly stochastic controlled system. A multimodal trajectory indicates instability, or a broad initial state distribution that yields several optimal trajectories. Also, it is ‘conjugate’ to quadratic costs (Section III-A), a widely applicable cost function class. Moreover, Gaussian filtering and smoothing has several attractive computational qualities, namely exact inference in the linear setting, and well-developed approximate message passing techniques in the nonlinear setting [49], [54], [55]. Finally, Gaussians are convenient to marginalize and condition on, such that $p(\mathbf{u}|\mathbf{x})$ results in time-varying linear (Gaussian) controllers. Therefore, while the Gaussian assumption is limiting, its locally linear quadratic approximations can be compared to linear quadratic optimal control approaches, which have been widely adopted.

DEFINITION 2: GAUSSIAN I2C INFERENCE

Control, where $\boldsymbol{\pi}_t(\mathbf{x}) = \mathcal{N}(\mathbf{K}_t^\pi \mathbf{x} + \mathbf{k}_t^\pi, \boldsymbol{\Sigma}_t^\pi)$

$$\mathbf{K}_t^\pi := \boldsymbol{\Sigma}_{\mathbf{u}\mathbf{x}_t} \boldsymbol{\Sigma}_{\mathbf{x}_t}^{-1} \quad (14)$$

$$\mathbf{k}_t^\pi := \boldsymbol{\mu}_{\mathbf{u}_t} - \mathbf{K}_t^\pi \boldsymbol{\mu}_{\mathbf{x}_t}$$

$$\boldsymbol{\Sigma}_t^\pi := \boldsymbol{\Sigma}_{\mathbf{u}_t} - \boldsymbol{\Sigma}_{\mathbf{u}\mathbf{x}_t} \boldsymbol{\Sigma}_{\mathbf{x}_t}^{-1} \boldsymbol{\Sigma}_{\mathbf{x}\mathbf{u}_t}^\top \quad (15)$$

$$\boldsymbol{\mu}_{\mathbf{u}_{t|\pi}} = \mathbf{K}_t^\pi \boldsymbol{\mu}_{\mathbf{x}_{t|\mathbf{f}}} + \mathbf{k}_t^\pi$$

$$\boldsymbol{\Sigma}_{\mathbf{u}_{t|\pi}} = \boldsymbol{\Sigma}_t^\pi + \mathbf{K}_t^\pi \boldsymbol{\Sigma}_{\mathbf{x}_{t|\mathbf{f}}} \mathbf{K}_t^{\pi\top}$$

Forward optimization (innovation from the cost)

$$p(\boldsymbol{\tau}_{t|\pi}) = p(\mathbf{x}_t, \mathbf{u}_t | \mathbf{z}_{1:t-1}) = \mathcal{N}\left(\begin{bmatrix} \boldsymbol{\mu}_{\mathbf{x}_{t|\mathbf{f}}} \\ \boldsymbol{\mu}_{\mathbf{u}_{t|\pi}} \end{bmatrix}, \begin{bmatrix} \boldsymbol{\Sigma}_{\mathbf{x}_{t|\mathbf{f}}} & \boldsymbol{\Sigma}_{\mathbf{x}_{t|\mathbf{f}}} \mathbf{K}_t^{\pi\top} \\ \mathbf{K}_t^\pi \boldsymbol{\Sigma}_{\mathbf{x}_{t|\mathbf{f}}} & \boldsymbol{\Sigma}_{\mathbf{u}_{t|\pi}} \end{bmatrix}\right)$$

$$\mathbf{z}_{t|\pi} = \mathbf{h}_t(\boldsymbol{\tau}_{t|\pi}) + \boldsymbol{\xi}_t$$

$$p(\mathbf{z}_{t|\pi}, \boldsymbol{\tau}_{t|\pi}) = \mathcal{N}\left(\begin{bmatrix} \boldsymbol{\mu}_{\mathbf{z}_{t|\pi}} \\ \boldsymbol{\mu}_{\boldsymbol{\tau}_{t|\pi}} \end{bmatrix}, \begin{bmatrix} \boldsymbol{\Sigma}_{\mathbf{z}_{t|\pi}} & \boldsymbol{\Sigma}_{\mathbf{z}_{t|\pi}} \mathbf{K}_t^{\pi\top} \\ \boldsymbol{\Sigma}_{\boldsymbol{\tau}_{t|\pi}} & \boldsymbol{\Sigma}_{\boldsymbol{\tau}_{t|\pi}} \end{bmatrix}\right) \quad (16)$$

$$\mathbf{K}_t^C := \boldsymbol{\Sigma}_{\boldsymbol{\tau}_{t|\pi}} \boldsymbol{\Sigma}_{\mathbf{z}_{t|\pi}}^{-1} \quad (\text{Kalman gain}),$$

$$\boldsymbol{\mu}_{\boldsymbol{\tau}_{t|C}} = \boldsymbol{\mu}_{\boldsymbol{\tau}_{t|\pi}} + \mathbf{K}_t^C (\mathbf{z}_t - \boldsymbol{\mu}_{\mathbf{z}_{t|\pi}})$$

$$\boldsymbol{\Sigma}_{\boldsymbol{\tau}_{t|C}} = \boldsymbol{\Sigma}_{\boldsymbol{\tau}_{t|\pi}} - \mathbf{K}_t^C \boldsymbol{\Sigma}_{\mathbf{z}_{t|\pi}} \mathbf{K}_t^{C\top}$$

Dynamics prediction, where $\mathbf{x}_{t+1|\mathbf{f}} = \mathbf{f}_t(\boldsymbol{\tau}_t) + \boldsymbol{\eta}_t$

$$p(\mathbf{x}_{t+1|\mathbf{f}}, \boldsymbol{\tau}_t) = \mathcal{N}\left(\begin{bmatrix} \boldsymbol{\mu}_{\mathbf{x}_{t+1|\mathbf{f}}} \\ \boldsymbol{\mu}_{\boldsymbol{\tau}_{t|C}} \end{bmatrix}, \begin{bmatrix} \boldsymbol{\Sigma}_{\mathbf{x}_{t+1|\mathbf{f}}} & \boldsymbol{\Sigma}_{\mathbf{x}_{t+1|\mathbf{f}}} \mathbf{F}_t^\top \\ \boldsymbol{\Sigma}_{\mathbf{x}_{t+1|\mathbf{f}}} \boldsymbol{\tau}_{t|C} & \boldsymbol{\Sigma}_{\boldsymbol{\tau}_{t|C}} \end{bmatrix}\right) \quad (17)$$

Backward optimization (smoothing)

$$\mathbf{K}_t^s := \boldsymbol{\Sigma}_{\boldsymbol{\tau}_{t|C}} \boldsymbol{\Sigma}_{\mathbf{x}_{t+1|\mathbf{f}}}^{-1}$$

$$\boldsymbol{\mu}_{\boldsymbol{\tau}_t|T} = \boldsymbol{\mu}_{\boldsymbol{\tau}_t|C} + \mathbf{K}_t^s (\boldsymbol{\mu}_{\mathbf{x}_{t+1|T}} - \boldsymbol{\mu}_{\mathbf{x}_{t+1|\mathbf{f}}})$$

$$\boldsymbol{\Sigma}_{\boldsymbol{\tau}_t|T} = \boldsymbol{\Sigma}_{\boldsymbol{\tau}_t|C} + \mathbf{K}_t^s (\boldsymbol{\Sigma}_{\mathbf{x}_{t+1|T}} - \boldsymbol{\Sigma}_{\mathbf{x}_{t+1|\mathbf{f}}}) \mathbf{K}_t^{s\top} \quad (18)$$

In Definition 2, we describe the explicit message passing for Gaussian I2C from Definition 1. To compactly delineate each step, we use $t|\pi$, $t|C$ and $t|\mathbf{f}$ to indicate a state after control, cost innovation and dynamics respectively. See Figure

1 for a factor graph visualization of the messages. As with standard Bayesian smoothing notation, t and $t|T$ describes the prior and posterior distribution. The initial state distribution is $\mathbf{x}_{1|\mathbf{f}} \sim p(\mathbf{x}_1)$. Note, the computation of the joint distributions (Equations 16 and 17) depends on the chosen message passing method, which is approximate in the nonlinear setting (Section III-E). While Equations 14-18 are familiar to those experienced in Gaussian state estimation, it is not immediately clear from the expressions that this computation performs optimal control. To reveal this, we must consider the linear Gaussian setting and its duality to linear quadratic optimal control.

D. The Linear Gaussian Setting

In the the case when dynamics \mathbf{f} and cost transform \mathbf{h} are affine transformations, the Gaussian message passing described in Section III-C can be performed exactly. Specifically, for notational simplicity we consider $C_t(\boldsymbol{\tau}) = \|\boldsymbol{\tau}_t^* - \boldsymbol{\tau}\|_{C_t}^2$, and $\mathbf{x}_{t+1} = \mathbf{F}_t \boldsymbol{\tau}_t + \bar{\mathbf{f}} + \boldsymbol{\eta}_t$ as in Section II-A.

Exact message passing allows us to examine the inference computation in closer detail, and therefore concretely derive the correspondence to optimal control. However, in order to do this, we must first carefully distinguish the prior, likelihood and posterior, where the prior is the filtered distribution and the posterior is the smoothed distribution¹. Adopting notation from previous work [13], [49], we use \rightarrow for the prior and \leftarrow for the likelihood, so the posterior $p(\mathbf{x}) \propto p(\overrightarrow{\mathbf{x}})p(\overleftarrow{\mathbf{x}})$, where

$$\boldsymbol{\Sigma} = (\overrightarrow{\boldsymbol{\Lambda}} + \overleftarrow{\boldsymbol{\Lambda}})^{-1} = \overrightarrow{\boldsymbol{\Sigma}} - \overrightarrow{\boldsymbol{\Sigma}} (\overrightarrow{\boldsymbol{\Sigma}} + \overleftarrow{\boldsymbol{\Sigma}})^{-1} \overrightarrow{\boldsymbol{\Sigma}}, \quad (19)$$

Clearly recovering the optimal control expressions from the messages is challenging due to the nested regularization provided by the probabilistic computation. Previous work [13], [15], [16] presents a Riccati equation view based on LQR. Here, we use the relation between the Q function and state-action log-likelihood as a compact alternative. To demonstrate this control equivalence, in the following passage we consider the limit where the prior becomes ‘uninformative’, that is $p(\mathbf{x}) \rightarrow p(\overleftarrow{\mathbf{x}})$, and the dynamics deterministic ($\boldsymbol{\Sigma}_{\boldsymbol{\eta}_t} \rightarrow \mathbf{0}$). Numerically, uninformative priors occur when the relative uncertainty in the prior is significantly larger than the likelihood. We use \rightarrow in the following expressions to express this limiting case. Revisiting the smoothing step (18), using Woodbury’s inversion lemma [56], we can express the posterior using Equation 19 as

$$\boldsymbol{\Sigma}_{\mathbf{x}_{t+1|T}} = \boldsymbol{\Sigma}_{\mathbf{x}_{t+1|\mathbf{f}}} - \boldsymbol{\Sigma}_{\mathbf{x}_{t+1|\mathbf{f}}} (\boldsymbol{\Sigma}_{\mathbf{x}_{t+1|\mathbf{f}}} + \boldsymbol{\Sigma}_{\mathbf{x}_{t+1|\leftarrow}})^{-1} \boldsymbol{\Sigma}_{\mathbf{x}_{t+1|\mathbf{f}}}.$$

Substituting into the smoothing update (Equation 18),

$$\boldsymbol{\Sigma}_{\boldsymbol{\tau}_t|T} = \boldsymbol{\Sigma}_{\boldsymbol{\tau}_t|C} - \boldsymbol{\Sigma}_{\boldsymbol{\tau}_t|C} \mathbf{F}_t^\top (\boldsymbol{\Sigma}_{\mathbf{x}_{t+1|\mathbf{f}}} + \boldsymbol{\Sigma}_{\mathbf{x}_{t+1|\leftarrow}}) \mathbf{F}_t \boldsymbol{\Sigma}_{\boldsymbol{\tau}_t|C}.$$

given $\mathbf{K}_t^s = \boldsymbol{\Sigma}_{\boldsymbol{\tau}_t|C} \mathbf{F}_t^\top \boldsymbol{\Sigma}_{\mathbf{x}_{t+1|\mathbf{f}}}^{-1}$ in the linear Gaussian setting. For affine dynamics, $\boldsymbol{\Sigma}_{\mathbf{x}_{t+1|\mathbf{f}}} = \mathbf{F}_t \boldsymbol{\Sigma}_{\boldsymbol{\tau}_t|C} \mathbf{F}_t^\top + \boldsymbol{\Sigma}_{\boldsymbol{\eta}_t}$, so we can use a matrix inversion identity² [56] for $\boldsymbol{\Lambda}_{\boldsymbol{\tau}_t|T}$, where

$$\boldsymbol{\Lambda}_{\boldsymbol{\tau}_t|T} = \boldsymbol{\Lambda}_{\boldsymbol{\tau}_t|C} + \mathbf{F}_t^\top (\boldsymbol{\Sigma}_{\boldsymbol{\eta}_t} + \boldsymbol{\Sigma}_{\mathbf{x}_{t+1|\leftarrow}})^{-1} \mathbf{F}_t. \quad (20)$$

¹This description does not fully match the Bayesian philosophy, as the prior should not depend on the data. However, it holds in the case of recursive Bayesian inference when considering a single timestep in isolation.

² $\mathbf{A}^{-1} - \mathbf{A}^{-1} \mathbf{U} (\mathbf{V} \mathbf{A}^{-1} \mathbf{U} + \mathbf{B}^{-1})^{-1} \mathbf{V} \mathbf{A}^{-1} = (\mathbf{A} + \mathbf{U} \mathbf{B} \mathbf{V})^{-1}$

The future state posterior can also be expressed as $\Sigma_{x_{t+1|T}} = (\Sigma_{x_{t+1|f}}^{-1} + \Sigma_{x_{t+1|e}}^{-1})^{-1}$, and given the uninformative prior $\Lambda_{x_{t+1|T}} \rightarrow \Lambda_{x_{t+1|e}}$. Moreover, from the innovation step during filtering $\Lambda_{\tau_t|C} = \Lambda_{\tau_t|\pi} + \alpha C_t$, and assuming Σ_{η_t} is negligible, Equation 20 reduces to

$$\Lambda_{\tau_t|T} \rightarrow \alpha C_t + F_t^\top \Lambda_{x_{t+1|T}} F_t, \quad (21)$$

since $\Lambda_{\tau_t|\pi}$ is uninformative. We can now identify Equation 21 as the Q update from Equation 5, with $\Lambda_{\tau_t|T} \equiv Q_t$ and $\Lambda_{x_{t+1|T}} \equiv V_t$. Reflecting on the deterministic dynamics assumption where Σ_{η_t} is negligible, the reader may recognize that the $(\Sigma_{\eta_t} + \Sigma_{x_{t+1|e}})^{-1} \rightarrow \Lambda_{x_{t+1|T}}$ step is the same regularization introduced to the value function in the risk-sensitive formulation in Section II-B, $V_t^\sigma = (\Sigma_{\eta_t} + \frac{1}{\sigma} V_t^{-1})^{-1}$. We discuss this correspondence in more detail in Section III-G.3.

Having shown that the Gaussian posteriors relate to Q and V , we now illustrate the maximization step of dynamic programming through marginalization. For brevity, we drop the time index and conditioning indicator. To relate the conditional of the τ precision to the optimal linear feedback law, consider the block-wise inversion of the joint covariance

$$\begin{aligned} \Lambda_\tau &= \begin{bmatrix} \Sigma_x & \Sigma_{ux}^\top \\ \Sigma_{ux} & \Sigma_u \end{bmatrix}^{-1} = \begin{bmatrix} \Lambda_{xx} & \Lambda_{xu} \\ \Lambda_{ux} & \Lambda_{uu} \end{bmatrix} \\ &= \begin{bmatrix} \Sigma_x^{-1} + \Sigma_x^{-1} \Sigma_{ux} \Sigma_*^{-1} \Sigma_{ux} \Sigma_x^{-1} & \Sigma_x^{-1} \Sigma_{ux}^\top \Sigma_*^{-1} \\ -\Sigma_*^{-1} \Sigma_{ux} \Sigma_x^{-1} & \Sigma_*^{-1} \end{bmatrix} \end{aligned} \quad (22)$$

where $\Sigma_* = \Sigma_u - \Sigma_{ux} \Sigma_x^{-1} \Sigma_{ux}^\top$ (Schur complement), so

$$\begin{aligned} -\Lambda_{uu}^{-1} \Lambda_{ux} &\equiv -Q_{uu}^{-1} Q_{ux}, \\ &= \Sigma_*^{-1} \Sigma_{ux} \Sigma_x^{-1} = \Sigma_{ux} \Sigma_x^{-1}. \end{aligned} \quad (23)$$

Therefore, Equation 23 relates the Q function-derived controller from Equation 6 to the i2C controller in Equation 14.

Finally, we use the joint precision in Equation 22 again to derive the value function update from Equation 7. The value function corresponds to the marginal of x from the joint. To understand its connection to the Q function, we consider the how the joint precision term Λ_{xx} in Equation 22 relates to the *marginal* state precision $\Sigma_x^{-1} = \Lambda_x$,

$$\Lambda_{xx} = \Sigma_x^{-1} + \Sigma_x^{-1} \Sigma_{ux} \Sigma_*^{-1} \Sigma_{ux} \Sigma_x^{-1} \quad (24)$$

$$= \Lambda_x + \Lambda_{xu} \Lambda_{uu}^{-1} \Lambda_{ux},$$

$$\therefore \Lambda_x = \Lambda_{xx} - \Lambda_{xu} \Lambda_{uu}^{-1} \Lambda_{ux}, \quad (25)$$

which corresponds to the V function update in Equation 7. As the dynamic programming method maintains a separate value and Q function, the value function is updated according to the equations in Equation 7. However, through manipulating the Gaussian distributions we can simply marginalize x from τ and compute Λ_x directly, and by working with the joint distribution throughout we avoid computing Q and V separately.

E. The Nonlinear Gaussian Setting

In this section, we review methods for Gaussian message passing when the exact linear rules are not possible. To briefly discuss the consequences for nonlinear systems in the context of the Section III-D analysis, we revisit the limiting assumption in Equation 21, and replace $h_t(\tau_t)$ with a locally

linear approximation $H_t \tau_t + \bar{h}_t$, which may be obtained via function linearization or ‘statistical linearization’ using the quadrature or sample estimates. Using this linearized model, our equivalent cost coefficients should be transformed for optimizing τ , i.e. $C_t^\tau = H^\top C_t H$. Starting from the simplified Kalman update of $\Sigma_{\tau_t|C}$, using the matrix inverse identity², we derive

$$\begin{aligned} \Sigma_{\tau_t|C} &= \Sigma_{\tau_t|\pi} - \Sigma_{\tau_t|\pi} H_t^\top (H \Sigma_{\tau_t|\pi} H_t^\top + \frac{1}{\alpha} C_\tau^{-1})^{-1} H_t \Sigma_{\tau_t|\pi} \\ \Lambda_{\tau_t|C} &= \Lambda_{\tau_t|\pi} + \alpha H_t^\top C_\tau H_t, \end{aligned} \quad \text{as expected.}$$

We now review available techniques for nonlinear Gaussian inference, which are visualized in Figure 2.

1) *Linearization*: Approximating the dynamics with a local linearization is attractive as it allows the linear Gaussian message passing rules to be adopted. Methods that adopt this approximation, such as the extended Kalman filter, are popular due to this convenience [57]. Like with DDP, a second-order approximation can also be used, though this is costly. Local linearization approximations are limited in their accuracy, not only for highly nonlinear systems, but also for large state uncertainties. They typically require greater regularization or iterative computation to refine the linearization point. Moreover, while Jacobians can be straightforward to calculate, due to advancements in automatic differentiation, they are still $F_t \in \mathbb{R}^{d_x \times d_\tau}$ objects and therefore expensive to evaluate without optimized implementations. Linearization is also brittle numerically when applied to discontinuities such as constraints. Also, as with iLQR, EM with the linearization-based inference corresponds to Gauss-Newton optimization [58].

2) *Spherical Cubature Quadrature*: In order to evaluate the integrals in Section III-B for Gaussian distributions, we can instead consider quadrature methods. Quadrature rules construct evaluation points and weights in order to evaluate integrals for specific functions, and for Gaussian densities the 3rd order spherical cubature rule is popular [59], as its complexity scales gracefully with dimensionality. This rule is also a special case of the unscented transform, popularized by the unscented Kalman filter [60]. The cubature quadrature rules are derived by computing points about the mean in each axis via the Cholesky decomposition of the covariance (sigma points). For computing the message rules for $y = f(x)$, $x \sim \mathcal{N}(\mu_x, \Sigma_x)$,

$$\begin{aligned} \tilde{x}_1^N &= \mu_x + \sqrt{d_x \Sigma_x} [\mathbf{I} - \mathbf{I}], \quad N = 2d_x, \quad w_n = \frac{1}{N}, \\ \mu_y &= \sum_n w_n f(\tilde{x}_n), \\ \Sigma_y &= \sum_n w_n (f(\tilde{x}_n) - \mu_y)(f(\tilde{x}_n) - \mu_y)^\top, \\ \Sigma_{yx} &= \sum_n w_n (f(\tilde{x}_n) - \mu_y)(\tilde{x}_n - \mu_x)^\top, \end{aligned}$$

where $\sqrt{\Sigma_x}$ is the lower-triangular Cholesky decomposition. The unscented transform includes the mean, and therefore as $2d_x + 1$ points, as well as two additional hyperparameters. While the unscented transform may provide an additional performance boost with hyperparameter tuning, we omit evaluation here and focus on the spherical cubature rules. Moreover, this rule relates to linearization through a finite difference approximation of the Jacobian via the sigma points, but crucially avoids computing the linearization explicitly [61].

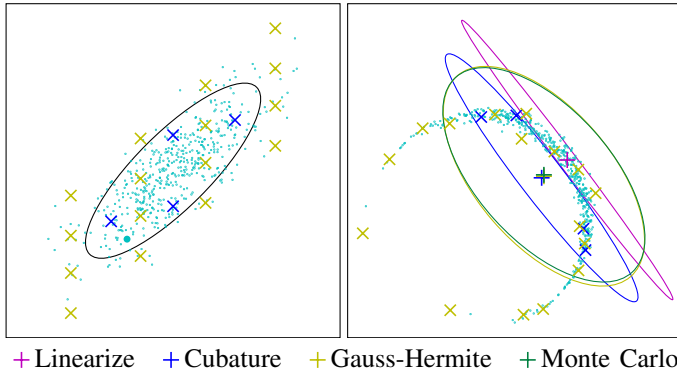


Fig. 2: An illustration of different approximate inference methods when propagating a bivariate Gaussian through a nonlinear function. The Monte Carlo samples (•) indicate the distribution becomes highly non-Gaussian, but evaluating these samples is computationally intensive. Linearizing the function returns an approximation that is highly localized around its (inaccurate) mean prediction. Cubature quadrature (+) uses $2d$ points, but improves the estimate, particularly in the mean. 4th-degree Gauss-Hermite (+) uses d^4 points, but almost directly matches the Monte Carlo estimate in mean and covariance.

3) Gauss-Hermite Quadrature: While state estimation requires computationally efficient inference methods for real-time use, for ‘offline’ trajectory optimization we are able to invest computational cost for greater inference accuracy. There are many approaches for achieving this for Gaussian distributions. For example, Monte Carlo sampling will converge, regardless of state dimension, due to the central limit theorem. However, for time-series inference sequential Monte Carlo methods are preferred, and in practice we did not find the Monte Carlo inference to be numerically reliable for the desired planning horizons. Continuing with the use of quadrature rules, Gauss-Hermite (G-H) rules [62] are designed integrals of the form $\int \exp(x^2)f(x)dx$, therefore appropriate for computing Gaussian moments. These rules are practically limited in the multivariate setting, as extending the quadrature points to a mesh results in exponential increase in points, d^p for state dimension d and degree p . We use it here as a baseline for accurate inference with i2C. The G-H message passing is the same as cubature quadrature, however the points and weights for a given degree must be obtained. Moreover, in the multivariate settings, the (1D) points and weights must be transformed to the appropriate mesh structure [55].

F. Expectation Maximization for Control

In the E-step, the Bayesian smoothing procedure returns an estimate of the optimal latent state-action distribution using the expected log-likelihood. The remaining unknown in the graphical model is the inverse temperature of the cost likelihood, α . While previous approaches treat this term as a fixed hyperparameter [16], [22], or derived from an explicit KL constraint [31], we treat it as an unknown model parameter which we can optimize in the M-step of EM. For Gaussian i2C, this expected log-likelihood is convex in α (Equation 27),

which affords the closed-form update [13],

$$\alpha = \frac{(T-1)d_z + d_{z_T}}{\sum_t \text{tr}\{\Theta_t \mathbb{E}[\delta z_t \delta z_t^\top]\}}, \text{ where } \delta z_t = z_t^* - z_t. \quad (26)$$

As $\text{tr}\{\Theta_t \mathbb{E}[\delta z_t \delta z_t^\top]\} = \mathbb{E}[\delta z_t^\top \Theta_t \delta z_t]$, the α update calibrates against the average trajectory cost over the belief, time horizon and state dimensionality. During the M-step, we also update the priors with the posterior $p(\mathbf{X}, \mathbf{U} | \mathbf{Z})$ for the next iteration.

In the nonlinear setting, this M-step is approximate as $\mathbb{E}[\delta z_t \delta z_t^\top]$ is estimated. Motivated by the idea of a regularized M-step, we restrict the update of α by applying a KL constraint to ξ , which can be shown to be equivalent to a ratio constraint on the α update [13]. As α is an inverse temperature, it controls the sharpness of the likelihood. For deterministic settings, this sharpness can be used to effectively optimize the objective. However, in the stochastic setting a sharp likelihood can greedily optimize for the random disturbances, as the ‘signal-to-noise ratio’ makes it difficult to optimize the controls under the stochastic dynamics. This tendency exploit uncertainty during optimization is coined ‘optimism’ [25]. Failing to regularize α can result in overly optimistic optimization, which may be numerically unstable (in the deterministic setting) or lead to violations of the dynamics (in the stochastic setting).

The complete i2C algorithm is summarized in Algorithm 1. The remaining hyperparameters to discuss are the control priors, specified for \mathbf{u} . These priors play a range of roles in the trajectory optimization and should be designed appropriately. Firstly they act as a learning rate, so lower variance priors will result in slower optimization. Secondly, they represent a source of entropy, so the variance also dictates the amount of possible exploration during optimization. Another design consideration is the nonlinearity of the system and inference choice, as the prior should be chosen to maintain the validity of the Gaussian assumption. Moreover, while i2C still works when the controls are initialized from zero mean (unlike DDP methods), it can take many iterations for the priors to ‘warm up’, therefore in practice (like in DDP methods) we initialize the control means with small Gaussian noise to accelerate optimization.

Regarding convergence guarantees, EM achieves monotonic improvement when inference is exact, and will converge to a unique optimum when the likelihood is convex [63]. When the E-step is approximate, likelihood optimality guarantees are limited by the inference accuracy [64]. This limitation motivates the adoption of Monte Carlo methods, as accuracy can be improved through a greater number of particles [52].

To discuss the computational complexity of Gaussian i2C, it depends on the choice of inference method, but ultimately rest on the matrix inversions of the largest covariance and the cost of evaluating the dynamics and cost function. As the covariance inversion can be framed as solving a linear system with a positive definite matrix, the complexity is reduced. Table II proves an empirical study of computational complexity for a complex dynamical system.

Finally, while this article focuses on optimal control, i2C is capable of performing alternative stochastic control approaches. For example, covariance control [65] can be easily implemented by applying the desired terminal state distribution during message passing [14].

EXPECTED LOG-LIKELIHOOD OF GAUSSIAN INPUT INFERENCE FROM CONTROL

$$-2\mathbb{E}[\mathcal{L}(\mathbf{X}_1^T, \mathbf{U}_1^{T-1}, \mathbf{Z}_1^T, \alpha)] = (d_{z_T} + (T-1)d_z + Td_x) \log 2\pi + \alpha \mathbb{E}[\|\mathbf{z}_T^* - \mathbf{h}_T(\mathbf{x}_T)\|_{\Theta_T}^2] + \alpha \sum_{t=1}^{T-1} \mathbb{E}[\|\mathbf{z}_t^* - \mathbf{h}_t(\mathbf{x}_t, \mathbf{u}_t)\|_{\Theta_t}^2] + \sum_{t=1}^{T-1} \mathbb{E}[\|\mathbf{x}_{t+1} - \mathbf{f}_t(\mathbf{x}_t, \mathbf{u}_t)\|_{\Sigma_{\eta_t}^{-1}}^2] + \mathbb{E}[\|\mathbf{x}_1 - \mu_{\mathbf{x}_1}\|_{\Sigma_{\mathbf{x}_1}^{-1}}^2] + \log |\Sigma_{\mathbf{x}_1}| + \sum_{t=1}^{T-1} \log |\Sigma_{\eta_t}| - \sum_{t=1}^T \log |\alpha \Theta_t| \quad (27)$$

G. Understanding Inference-based Control

Having demonstrated Gaussian smoothing performs optimal control, we now discuss the additional benefits of inference-based control. This is illustrated in the expected log-likelihood objective (27) which, while an upper bound of the control objective, contains additional regularization terms which can be connected to prior methods in control.

1) Maximum Entropy Regularization: The Gaussian assumption naturally incorporates its log normalization terms into the log-likelihood, which for the Gaussian distribution is also its negative entropy. Augmenting the control objective with entropies evokes the maximum entropy principle (ME), which as been applied to control for robustness, in particular for the controller in inverse optimal control [66]. The latent Gaussian prior on controls therefore induces a natural ME effect on i2C, which can be derived by examining the posterior policy. In explicit ME iLQG, the policy covariance takes the form $\Sigma_t = (\mathbf{C}_{\mathbf{u}_t} + \mathbf{F}_{\mathbf{u}_t}^\top \mathbf{V}_{t+1} \mathbf{F}_{\mathbf{u}_t})^{-1}$ [67]. We can see from Q update in Equation 5 that this is the inverse of $\mathbf{Q}_{\mathbf{u}_t}$, and the expression for $\Sigma_{\mathbf{u}_t}$ in i2C (Equation 15) corresponds to the Schur complement form of $\Lambda_{\mathbf{u}_t}$ in Equation 22.

As the stochastic aspect of the linear Gaussian controller is undesired in practice, the value of this ME regularization could be questioned. However, ME regularization was observed to influence desirable optimization behavior. For robust regions (e.g. where controls are clamped), the control variance was large, whereas at sensitive regimes (e.g. during energy injection in swing-up tasks) this variance was at a minimum. When updating \mathbf{u} using Bayes rule, a lower variance prior reduces the size of updates, therefore we suggest the ME effect on i2C identifies robust and sensitive regions of the trajectory and regularizes the update rates to the controls accordingly.

2) Uncertainty-based Regularization: An important aspect to i2C is how uncertainty influences the optimized control law. Most notable from Equation 14 is how the gain is attenuated by $\Sigma_{\mathbf{x}_t}$, indicating that control action reduces with state uncertainty. This finding parallels the ‘turn-off phenomenon’ observed in dual control [68], [69] and Bayesian reinforcement learning [70], where actions are similarly attenuated under model uncertainty. For dual control, this regularization is detrimental due to the active learning component, however this behavior is useful in settings such as model-based reinforcement learning [12], where regions of predictive uncertainty can indicate modeling error, and uncertainty-based regularization prevents these errors being exploited during optimization [71].

3) Risk-Seeking Optimization: Exponentiating the optimal control objective for risk sensitivity (Equation 8) has a clear connection to control-as-inference, due to the likelihood definition in Equation 10. As previous work has noted, this therefore relates the risk coefficient σ to the inverse temperature α [17], [26], [31]. An immediate consequence of this is that $\sigma > 0$ for control-as-inference, therefore it is inherently ‘risk seeking’. Characterizing risk-seeking behavior as control attenuation, we

can interpret this as a manifestation of the turn-off phenomena, as increasing σ acts to increase the state uncertainty. Interestingly, this presents risk-averse control as the opposite of the turn-off phenomena, artificially reversing the regularization through the sign reversal of σ . The artificial nature of this mechanism is reflected in the numerical brittleness of risk-averse control, as it requires $\Sigma_{\eta_t} + \frac{1}{\sigma} \mathbf{V}_t^{-1}$ to be positive definite when $\sigma < 0$, which is difficult to ensure.

On top of feedback regularization, i2C uses risk-seeking control in a secondary fashion due to the forward optimization during filtering. From the M-step update of i2C (Equation 26), we can see that as the average cost decreases, α increases and therefore the effective risk-seeking increases. To appreciate why σ must increase during optimization, and not simply remain fixed to a small (risk neutral) value, we must inspect the expected log-likelihood objective (Equation 27). We can see that α weighs the control objective in the overall likelihood, therefore a small α does not encourage exploration. Moreover, prematurely settings α high leads to overly aggressive forward optimization that neglects the dynamics constraint. Numerically, this manifests as aggressive filtering during the E-step, that greedily optimizes the cost-to-come during the forward pass. This ‘optimistic’ greediness (introduced in Section III-F), can prefer trajectories that violate the dynamics constraint, as $p(\mathbf{x}_{t+1} | \mathbf{x}_t, \mathbf{u}_t, \mathbf{z}_{1:t}) \neq p(\mathbf{x}_{t+1} | \mathbf{x}_t, \mathbf{u}_t)$ [25]. Conversely, the risk-neutral case effectively turns off this forward optimization, removing the beneficial exploration effect completely. Therefore, i2C leverages ‘risk seeking’ behavior to accelerate optimization and the M-step is crucial in tempering this exploration appropriately each iteration.

4) Optimism as Exploration: Comparing the dynamics constraint in Equation 1 against the complete likelihood objective in Equation 27, one is reminded of barrier methods for constrained optimization, as the dynamics constraint now takes the form of a quadratic penalty. This becomes interesting when Σ_{η_t} is not constant, as the constraint is relaxed as Σ_{η_t} increases. Like in dual control, the value in this behavior depends on whether we are considering statistical or model uncertainty. High statistical uncertainty corresponds to a challenging stochastic control problem, and we require careful tuning of α to avoid exploitation. Due to the turn-off phenomena, this setting is inherently challenging and will likely take many iterations to converge and requires accurate inference. Model uncertainty corresponds to dual control and model-based reinforcement learning. Here, the constraint relaxation is beneficial, as the optimization naturally guides the trajectory towards low cost trajectories where the model is uncertain. In contrast to dual control, this behavior does not seek to learn the model efficiently, but rather bias data collection towards low cost regions. This can be interpreted as a guided exploration strategy that could benefit the sample efficiency of data-driven control [12].

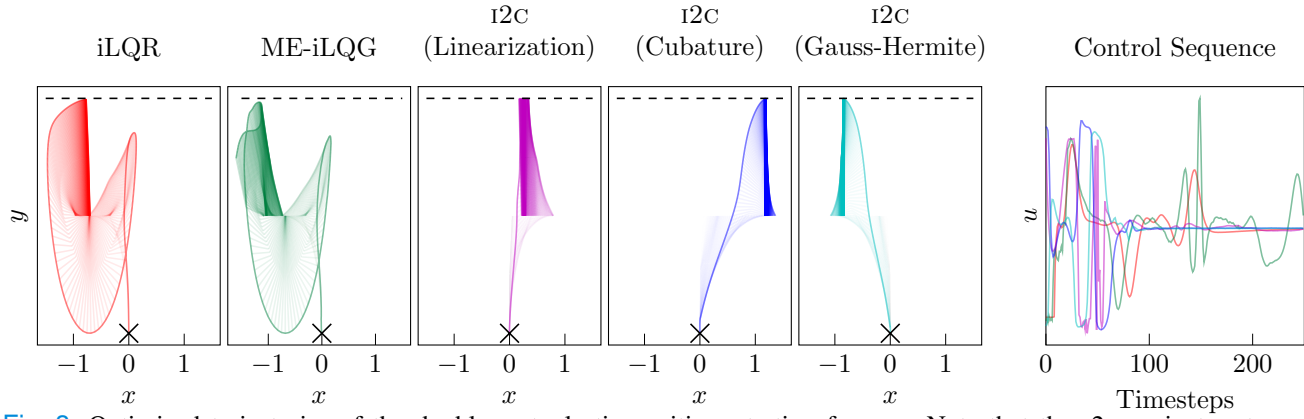


Fig. 3: Optimized trajectories of the double cartpole tip position, starting from \times . Note that the i2C variants return similar results due to shared hyperparameters. While the quadrature methods have cleaner trajectories due to the accuracy of their inference, that are remarkably similar given Gauss-Hermite requires much greater computation.

IV. EXTENSIONS

This section presents several improvements and extensions to i2C for the stochastic control setting.

A. Expert Linear Gaussian Controllers

A weakness of the Gaussian assumption made in Section III-C is the local nature of the estimate. Gaussian inference is equivalent to regularized local linearizations about the mean state-action trajectory. The local nature of this assumption introduces a brittleness to the control that limits its application in practical settings without additional modifications like replanning, a limitation it shares with linearization-based control algorithms. Using inference, we can leverage the state belief to reduce this brittleness. In statistical machine learning, an *expert* is a model whose appropriateness applies to a specific portion of a state space. We can incorporate this idea into the TV-LC by switching between open- and closed-loop control using the predicted state distribution, (Figure 4),

$$\pi_t(u|x) = \Pr(x_t=x) p(u_t|x_t=x) + \Pr(x_t \neq x) p(u_t). \quad (28)$$

For continuous random variables, $\Pr(x_t=x)$ is an awkward quantity to compute. We take inspiration from outlier detection and define a suitable confidence interval. For a multivariate Normal distribution, our $\Pr(x_t=x)$ can be computed using the Mahalanobis distance $d(x) = \|x - \mu_{x_t}\|_{\Sigma_{x_t}^{-1}}$, which has a chi-square distribution. Using the cumulative density function $F_{\chi_k^2}$, $\Pr(x_t=x) = 1 - F_{\chi_k^2}(d(x))$ [72]. For $k=2$,

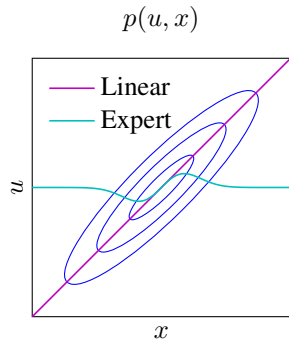


Fig. 4: Illustration of the conditional Gaussian distribution as a linear controller. The standard treatment holds even far outside the expected distribution. The ‘expert’ controller reverts to the prior when far from the mean, which prevents erroneous feedback control in regions where the controller was not designed for.

$\Pr(x_t=x) = \exp(-\frac{1}{2}d(x))$, which works well and is convenient to compute, as it is the unnormalized density of x_t .

While this expert controller is valuable during optimization, it can also be used in execution, as it provides a degree of ‘safety’ by turning off feedback. However, there are also situations where this feedback relaxation impedes performance, such as unstable systems where high feedback is critical.

B. Integrating State Estimation and Control

As i2C uses recursive Bayesian estimation, it can be integrated seamlessly with state estimation algorithms, which correspond to the partially-observed optimal control problem. In the linear Gaussian case, the separation principle applies and the combination of a Kalman filter and LQR controller is optimal. In the nonlinear setting, this convenient separation is no longer valid, however it is still applied in practice [44]. For i2C, the probabilistic graphical model is now extended to include a measurement model, i.e. $y_t = g_t(x) + \zeta_t$, $y \in \mathbb{R}^{d_y}$, $\zeta_t \sim \mathcal{N}(\mathbf{0}, \Sigma_\zeta)$ for the nonlinear Gaussian setting. Under this time-varying PGM, the past and present state distribution is now defined by the state estimation. Therefore, each timestep the control must be adapted to the updated state distribution. This replanning procedure naturally evokes model predictive control (MPC), which is also motivated by adapting optimal control to an evolving state distribution [73]. There is also a connection to dual control and the notion of closed-loop control vs. feedback control of Tse and Bar Shalom [74], as early work on replanning was motivated by reducing the adverse consequences of the turn-off phenomena (discussed in Section III-G.2) [74], [75].

V. SIMULATED EXPERIMENTS

This section provides benchmarks of the i2C algorithm described in Section III as a trajectory optimization solver, as well as empirical investigations into the extensions discussed in Section IV: Expert-controllers and partially-observed MPC.

A. Approximate Inference for Control

In Section III-E, several approximate Gaussian message passing methods were discussed in order to apply Gaussian i2C to nonlinear systems. For this experiment, we evaluate each method on a deterministic double cartpole swing-up

TABLE I: The evaluation of SOC algorithms on finite-horizon, input-constrained control tasks. Variations are characterized by optimizing the stochastic (S) or certainty equivalent (CE) setting and using open-loop (FF), closed-loop (FB) or expert (E) controllers during optimization. These features identify similarities in performance. Percentiles were computed from 100 rollouts. SQP combines an open-loop trajectory optimized with sequential quadratic programming with local LQR feedback.

Environment	10th, 90th Cost Percentiles ($\times 10^3$)								
	i2C (S, E)	i2C (CE, E)	i2C (S, FF)	i2C (S, FB)	i2C (CE, FF)	i2C (CE, FB)	SQP (CE, FF)	iLQR (CE, FB)	ME-iLQG (S, FB)
Pendulum	13.46, 21.53	12.81, 17.11	17.72, 21.94	19.23, 21.43	13.97, 26.77	19.49, 22.31	18.10, 26.31	23.33, 26.46	19.45, 20.91
Cartpole	85.06, 87.43	81.83, 83.87	89.53, 94.67	93.53, 95.71	86.93, 89.75	121.89, 123.88	111.31, 118.57	142.23, 145.78	120.80, 122.45

task. As a double cartpole is a chaotic nonlinear system, the degree of nonlinearity should challenge the accuracy of the approximate inference. As a baseline, we consider iLQR and maximum entropy iLQG (denoted ME-iLQG) [28], which use linearization-based approximations with line-search and relative entropy constrained updates respectively.

In order to demonstrate the consequences of approximate inference, we use the same priors and regularization across all i2C variants. In doing so, we show that i2C variations achieve similar high performance, but illustrate in Figure 5 how inference quality impacts optimization. Another important consideration is computation time. As discussed earlier, linearization-based approaches are unwieldy due to the Jacobian computation, especially for environments where Taylor approximation are not straightforward to compute. Moreover, iLQR requires line search for regularization which introduces additional computation. ME-iLQG uses cheaper, but usually conservative, KL regularization. The benefit of i2C is the adaptive regularization of the Bayes rule, which comes with the caveat of ‘optimistic exploration’. Moreover, the use of inference allows for greater flexibility in computation. Table II reports the average iteration time for double cartpole optimization. Note that the implementations of iLQR and ME-iLQG have optimized codebases, with pre-compiled Riccati equations and parallelized Jacobian computation. Despite this, iLQR is the most expensive, primarily due to the line search, as iterations were observed to be up to $\times 2$ faster than the average. ME-iLQG is faster than linearized i2C due to the ability to parallelize linearization, however cubature inference is the significantly faster method, as it balances computation and accuracy in a very attractive fashion in the nonlinear Gaussian setting. Moreover, while Gauss-Hermite inference is understandably the more expensive quadrature method, it was found to be faster than iLQR. Secondly, while G-H inference is

clearly more accurate than cubature (e.g. Figure 2), the results in Figures 3 and 5 show that for double cartpole cubature was sufficient accuracy.

B. Trajectory Optimization of Stochastic Systems

To evaluate the performance of the expert controller (Section IV-A), we consider two stochastic, nonlinear swing-up tasks against various open- and closed-loop baselines. The solvers also vary between considering the actual stochastic problem or a certainty equivalent approximation. In Table I we compare both i2C and baseline SOC solvers. For both tasks, open-loop methods resulted in better optima but were also high variance in the cost, while the closed-loop alternatives had much lower variance but sub-optimal performance on the simulated systems due to their over-actuation. Reassuringly, the results of the i2C variant and equivalent baseline solver were generally similar due to the comparable computation.

Incorporating the expert controller during optimization, it softens the feedback control during exploration, effectively acting open-loop. This avoids highly-actuated trajectories forming, avoiding local optima. Table I demonstrates the effectiveness of this addition, where this expert controller matches the open-loop optima but with the closed-loop variance reduction.

C. Model Predictive Control

To investigate i2C MPC with state estimation, we compare cubature Gaussian i2C with iLQR for an acrobatic quadcopter

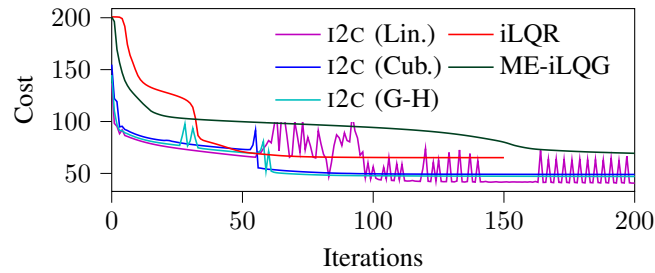


Fig. 5: Cost of the mean trajectory during trajectory optimization for double cartpole swing-up. While all i2C variance converge on similar solutions, the inaccuracy of linearization-based inference makes optimization more unstable.

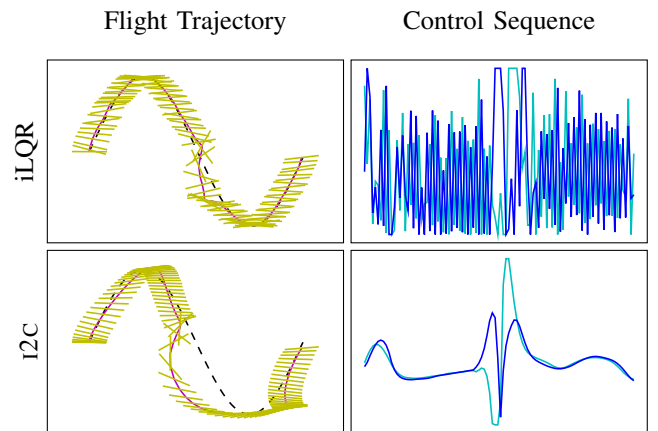


Fig. 6: Comparing the control of i2C and iLQR for an acrobatic quadrocopter task, consisting of a smooth trajectory and 360° flip, under high measurement noise ($\Sigma_\zeta^{\text{high}}$). The trajectory is depicted by the desired and achieved cartesian trajectory, along with the measured pose. The controls consist of two thrusts applied each end of the vehicle.

	iLQR	ME-iLQG	i2C (Lin.)	i2C (Cub.)	i2C (G-H)
Time (s)	1.0	0.21	0.35	0.03	0.69

TABLE II: Relative computation time per iteration for double cartpole trajectory optimization, averaged over ≤ 200 iterations and normalized about iLQR. G-H is degree 4.

task, using a cubature Kalman filter for state estimation. Tracking a pre-specified trajectory, we evaluate the performance across increasing measurement uncertainty using the measurement model from Section IV-B. To simulate interesting state estimation dynamics, the positions and velocities of the left and right side of the copter in the world frame are measured. Therefore, during the somersault (Figure 6) the state uncertainty fluctuates, as the state is observed in a nonlinear manner. We evaluate two measurement noise settings: low and high noise ($\Sigma_{\zeta}^{\text{low}}$, $\Sigma_{\zeta}^{\text{high}}$), where high noise masks out the velocities and right side position sensor. Low noise evaluates the methods for MPC, while the high noise case evaluates the effect of increased state uncertainty on i2C. iLQR is a deterministic, risk-neutral method, while i2C is probabilistic and risk-seeking, therefore we aim to understand how i2C uses of the state uncertainty from filtering and whether this aids control. Table III discusses the results.

VI. CONCLUSION

We have shown how input estimation can be used to frame optimal control as an inference problem. In doing so, we perform risk-seeking, maximum entropy stochastic control, and can adopt principled approximate inference methods for effective nonlinear optimization. While uncertainty-based regularization comes with (long-established) weaknesses, this approach has been demonstrated to be numerically competitive with popular solvers while also extending to alternative stochastic control methods like covariance control. Future work should consider relaxing the Gaussian assumption through methods such as sequential Monte Carlo [52], enabling multi-modal trajectory optimization and arbitrary objectives. Moreover, the inclusion of chance constraints [76] into the inference procedure would make an important addition towards i2C as a complete solver.

REFERENCES

- [1] P. Dayan and G. E. Hinton, “Using expectation-maximization for reinforcement learning,” *Neural Computation*, 1997.
- [2] H. Attias, “Planning by probabilistic inference,” in *Proc. of the 9th Int. Workshop on Artificial Intelligence and Statistics*, 2003.
- [3] M. Toussaint and A. Storkey, “Probabilistic inference for solving discrete and continuous state Markov Decision Processes,” in *International Conference of Machine Learning*, 2006.
- [4] H. J. Kappen, V. Gómez, and M. Opper, “Optimal control as a graphical model inference problem,” in *International Conference on Automated Planning and Scheduling*, 2013.
- [5] R. E. Kalman, “A new approach to linear filtering and prediction problems,” *Journal of basic Engineering*, 1960.
- [6] E. Todorov, “General duality between optimal control and estimation,” in *IEEE Conference on Decision and Control*, 2008.
- [7] E. Theodorou and E. Todorov, “Relative entropy and free energy dualities: Connections to path integral and KL control,” in *IEEE Conference on Decision and Control*, 2012.
- [8] P. Hennig, M. A. Osborne, and M. Girolami, “Probabilistic numerics and uncertainty in computations,” *Proceedings of the Royal Society A: Mathematical, Physical and Engineering Sciences*, 2015.
- [9] A. Mesbah, “Stochastic model predictive control: An overview and perspectives for future research,” *IEEE Control Systems Magazine*, vol. 36, no. 6, pp. 30–44, 2016.
- [10] N. Matni, A. Proutiere, A. Rantzer, and S. Tu, “From self-tuning regulators to reinforcement learning and back again,” in *IEEE Conference on Decision and Control*, 2019.
- [11] L. Hewing, K. P. Wabersich, M. Menner, and M. N. Zeilinger, “Learning-based model predictive control: Toward safe learning in control,” *Annual Review of Control, Robotics, and Autonomous Systems*, 2020.
- [12] M. P. Deisenroth, G. Neumann, J. Peters *et al.*, “A survey on policy search for robotics,” *Foundations and Trends® in Robotics*, 2013.
- [13] J. Watson, H. Abdulsamad, and J. Peters, “Stochastic optimal control as approximate input inference,” in *Conference on Robot Learning*, 2019.
- [14] J. Watson and J. Peters, “Advancing trajectory optimization with approximate inference: Exploration, covariance control and adaptive risk,” in *American Control Conference*, 2021.
- [15] C. Hoffmann and P. Rostalski, “Linear optimal control on factor graphs - a message passing perspective -,” *International Federation of Automatic Control*, 2017.
- [16] M. Toussaint, “Robot trajectory optimization using approximate inference,” in *International Conference on Machine Learning*, 2009.
- [17] K. C. Rawlik, “On probabilistic inference approaches to stochastic optimal control,” Ph.D. dissertation, The University of Edinburgh, 2013.
- [18] Y. Ho and R. Lee, “A bayesian approach to problems in stochastic estimation and control,” *IEEE Transactions on Automatic Control*, 1964.
- [19] G. Williams, A. Aldrich, and E. A. Theodorou, “Model predictive path integral control: From theory to parallel computation,” *Journal of Guidance, Control, and Dynamics*, 2017.
- [20] M. Hoffman, A. Doucet, N. Freitas, and A. Jasra, “Bayesian policy learning with trans-dimensional mcmc,” in *Advances in Neural Information Processing Systems*, 2008.
- [21] E. Todorov, “Linearly-solvable markov decision problems,” in *Advances in Neural Information Processing Systems*, 2007.
- [22] K. Rawlik, M. Toussaint, and S. Vijayakumar, “On stochastic optimal control and reinforcement learning by approximate inference,” in *International Joint Conference on Artificial Intelligence*, 2013.
- [23] J. Watson, “Control as inference? comparing path integral and message passing methods for optimal control,” *Reinforcement Learning Algorithms: Analysis and Applications*, 2021.
- [24] G. Neumann, “Variational inference for policy search in changing situations,” in *International Conference on Machine Learning*, 2011.
- [25] S. Levine, “Reinforcement learning and control as probabilistic inference: Tutorial and review,” *arXiv preprint arXiv:1805.00909*, 2018.
- [26] B. O’Donoghue, “Variational bayesian reinforcement learning with regret bounds,” *arXiv preprint arXiv:1807.09647*, 2018.
- [27] D. H. Jacobson and D. Q. Mayne, “Differential dynamic programming,” 1970.
- [28] S. Levine and V. Koltun, “Guided policy search,” in *International Conference on Machine Learning*, 2013.
- [29] R. Lioutikov, A. Paraschos, J. Peters, and G. Neumann, “Sample-based information-theoretic stochastic optimal control,” in *IEEE International Conference on Robotics and Automation*, 2014.

Algorithm	10th, 90th Cost Percentiles	
	$\Sigma_{\zeta}^{\text{low}}$	$\Sigma_{\zeta}^{\text{high}}$
i2C (FF)	40.59, 41.52	113.35, 125.96
i2C (FB)	39.98, 41.03	113.41, 126.02
iLQR (FF)	111.73, 1968.39	107.02, 1809.36
iLQR (FB)	48.67, 68.35	53.85, 73.33

TABLE III: Acrobatic quadrocopter tracking performance under increasing state uncertainty over 50 random seeds. In the low noise setting, the i2C controller is superior and consistent across control modes. In the high noise setting, the increased states uncertainty induces i2C to regularize the control, leading to an increased cost that surpasses iLQR, but with reduced spread. This task setting illustrates when uncertainty-based regularization can be detrimental to performance.

[30] H. Abdulsamad, O. Arenz, J. Peters, and G. Neumann, "State-regularized policy search for linearized dynamical systems," in *Proceedings of the International Conference on Automated Planning and Scheduling (ICAPS)*, 2017.

[31] S. Levine and V. Koltun, "Variational policy search via trajectory optimization," in *Advances in Neural Information Processing Systems*, 2013.

[32] M. Mukadam, C.-A. Cheng, X. Yan, and B. Boots, "Approximately optimal continuous-time motion planning and control via probabilistic inference," in *IEEE International Conference on Robotics and Automation*, 2017.

[33] M. Mukadam, J. Dong, X. Yan, F. Dellaert, and B. Boots, "Continuous-time gaussian process motion planning via probabilistic inference," *The International Journal of Robotics Research*, 2018.

[34] J. van den Berg, "Extended LQR: Locally-optimal feedback control for systems with non-linear dynamics and non-quadratic cost," in *Robotics Research*. Springer, 2016.

[35] W. Sun, J. van den Berg, and R. Alterovitz, "Stochastic extended LQR for optimization-based motion planning under uncertainty," *IEEE Transactions on Automation Science and Engineering*, 2016.

[36] E. Todorov and Y. Tassa, "Iterative local dynamic programming," in *Symposium on Adaptive Dynamic Programming and Reinforcement Learning*, 2009.

[37] Y. Tassa, T. Erez, and W. Smart, "Receding horizon differential dynamic programming," in *Advances in Neural Information Processing Systems*, 2008.

[38] Z. Manchester and S. Kuindersma, "Derivative-free trajectory optimization with unscented dynamic programming," in *IEEE Conference on Decision and Control*, 2016.

[39] T. Howell, C. Fu, and Z. Manchester, "Direct policy optimization using deterministic sampling and collocation," *IEEE Robotics and Automation Letters*, 2021.

[40] J. Rajamäki, K. Naderi, V. Kyrki, and P. Hämäläinen, "Sampled differential dynamic programming," in *IEEE International Conference on Intelligent Robots and Systems*, 2016.

[41] J. Rajamäki and P. Hämäläinen, "Regularizing sampled differential dynamic programming," in *American Control Conference*, 2018.

[42] A. E. Bryson, *Applied optimal control: Optimization, estimation and control*. Routledge, 2018.

[43] W. Li and E. Todorov, "Iterative linear quadratic regulator design for nonlinear biological movement systems," in *1st International Conference on Informatics in Control, Automation and Robotics*, 2004.

[44] E. Todorov and W. Li, "A generalized iterative LQG method for locally-optimal feedback control of constrained nonlinear stochastic systems," in *American Control Conference*, 2005.

[45] D. Jacobson, "Optimal stochastic linear systems with exponential performance criteria and their relation to deterministic differential games," *IEEE Transactions on Automatic Control*, 1973.

[46] P. Whittle, "Risk-sensitive linear/quadratic/gaussian control," *Advances in Applied Probability*, 1981.

[47] F. Farshidian and J. Buchli, "Risk sensitive, nonlinear optimal control: Iterative linear exponential-quadratic optimal control with gaussian noise," *arXiv preprint arXiv:1512.07173*, 2015.

[48] J. Peters and S. Schaal, "Reinforcement learning by reward-weighted regression for operational space control," in *International Conference on Machine Learning*, 2007.

[49] H.-A. Loeliger, J. Dauwels, J. Hu, S. Korl, L. Ping, and F. R. Kschischang, "The factor graph approach to model-based signal processing," *Proceedings of the IEEE*, 2007.

[50] R. H. Shumway and D. S. Stoffer, "An approach to time series smoothing and forecasting using the em algorithm," *Journal of time series analysis*, 1982.

[51] Z. Ghahramani and S. T. Roweis, "Learning nonlinear dynamical systems using an em algorithm," in *Advances in Neural Information Processing Systems*, 1999.

[52] T. B. Schön, A. Wills, and B. Ninness, "System identification of nonlinear state-space models," *Automatica*, 2011.

[53] L. Bruderer, "Input estimation and dynamical system identification: New algorithms and results," Ph.D. dissertation, ETH Zurich, 2015.

[54] E. Petersen, C. Hoffmann, and P. Rostalski, "On approximate nonlinear gaussian message passing on factor graphs," in *2018 IEEE Statistical Signal Processing Workshop*, 2018.

[55] S. Särkkä, *Bayesian Filtering and Smoothing*. Cambridge University Press, 2013.

[56] K. B. Petersen, M. S. Pedersen *et al.*, "The matrix cookbook," *Technical University of Denmark*, 2008.

[57] B. D. Anderson and J. B. Moore, *Optimal filtering*, 2012.

[58] B. M. Bell, "The iterated Kalman smoother as a Gauss–Newton method," *SIAM Journal on Optimization*, 1994.

[59] I. Arasaratnam and S. Haykin, "Cubature kalman filters," *IEEE Transactions on Automatic Control*, 2009.

[60] S. J. Julier and J. K. Uhlmann, "New extension of the Kalman filter to nonlinear systems," in *Signal Processing, Sensor Fusion, and Target Recognition VI*. International Society for Optics and Photonics, 1997.

[61] T. S. Schei, "A finite-difference method for linearization in nonlinear estimation algorithms," *Automatica*, 1997.

[62] K. Ito and K. Xiong, "Gaussian filters for nonlinear filtering problems," *IEEE Transactions on Automatic Control*, 2000.

[63] C. F. J. Wu, "On the Convergence Properties of the EM Algorithm," *The Annals of Statistics*, 1983.

[64] A. Gunawardana and W. Byrne, "Convergence theorems for generalized alternating minimization procedures," *Journal of Machine Learning Research*, 2005.

[65] A. F. Hotz and R. E. Skelton, "A covariance control theory," in *IEEE Conference on Decision and Control*, 1985.

[66] B. D. Ziebart, "Modeling purposeful adaptive behavior with the principle of maximum causal entropy," Ph.D. dissertation, Carnegie Mellon University, 2010.

[67] S. Levine, "Motor skill learning with local trajectory methods," Ph.D. dissertation, Stanford University, 2014.

[68] M. Aoki, *Optimization of stochastic systems: topics in discrete-time systems*. Academic Press, 1967, vol. 32.

[69] Y. Bar-Shalom, "Stochastic dynamic programming: Caution and probing," *IEEE Transactions on Automatic Control*, 1981.

[70] E. D. Klenkske and P. Hennig, "Dual control for approximate bayesian reinforcement learning," *Journal of Machine Learning Research*, 2016.

[71] J. G. Schneider, "Exploiting model uncertainty estimates for safe dynamic control learning," *Advances in Neural Information Processing Systems*, 1997.

[72] R. Johnson and D. Wichern, *Applied multivariate statistical analysis*, 2002.

[73] "Model predictive control: past, present and future," *Computers & Chemical Engineering*, 1999.

[74] Y. Bar-Shalom and E. Tse, "Dual effect, certainty equivalence, and separation in stochastic control," *IEEE Transactions on Automatic Control*, 1974.

[75] R. Curry, "A new algorithm for suboptimal stochastic control," *IEEE Transactions on Automatic Control*, 1969.

[76] B. L. Miller and H. M. Wagner, "Chance constrained programming with joint constraints," *Operations Research*, 1965.

APPENDIX

Experimental details can be found in the public codebase³.

³www.github.com/JoeMWatson/input-inference-for-control